Exploring Thermochromic Behavior of Hydrated Hybrid Perovskites in Solar Cells

ARTICLE *in* JOURNAL OF PHYSICAL CHEMISTRY LETTERS · JULY 2015

Impact Factor: 7.46 · DOI: 10.1021/acs.jpclett.5b01426

5 AUTHORS, INCLUDING:

Ansuman Halder
Indian Institute of Technology Bombay
6 PUBLICATIONS **53** CITATIONS
SEE PROFILE

Soham Ghosh
Indian Institute of Technology Bombay
7 PUBLICATIONS **57** CITATIONS
SEE PROFILE

Anand Selvin Subbiah
Indian Institute of Technology Bombay
14 PUBLICATIONS **65** CITATIONS
SEE PROFILE

THE JOURNAL OF PHYSICAL CHEMISTRY Letters

Letter

pubs.acs.org/JPCL

Exploring Thermochromic Behavior of Hydrated Hybrid Perovskites in Solar Cells

Ansuman Halder, Devika Choudhury, Soham Ghosh, Anand S. Subbiah, and Shaibal K Sarkar*

Department of Energy Science and Engineering, Indian Institute of Technology Bombay, Powai, Mumbai 400076, India

Supporting Information

ABSTRACT: Highly reproducible and reversible thermochromic nature of dihydrated methylammonium lead iodide is found. A wide bandgap variation of the material (~2 eV) is detected between room temperature and 60 °C under ambient condition as a result of phase transition caused by moisture absorption and desorption. In situ X-ray diffraction and Fourier transform infrared spectroscopy studies are performed to understand the mechanistic behavior during the phase transition. This thermochromic property is further explored as absorber material in mesostructured solar cells. Temperature-dependent reversible power conversion efficiency greater than 1% under standard test conditions is demonstrated; revealing its potential applicability in building integrated photovoltaics.

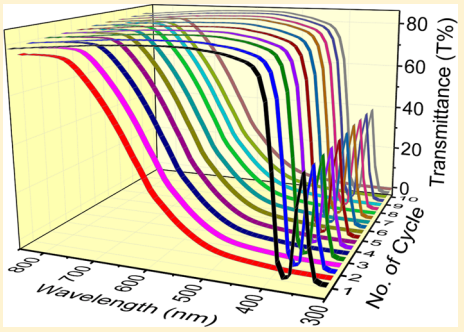

Hybrid molecular perovskite structures consisting of organic and inorganic submodules provide ample openings to tailor material properties for a variety of scientific and technological applications.[1] While the covalently bonded inorganic component determines the optoelectronic properties,[1,2] the organic components that are weakly bonded with their counterparts contribute to the plastic mechanical properties and structural diversity in the material.[1] One such combination, the hybrid organic−inorganic methylammonium lead halides ($CH_3NH_3PbX_3$; X: halide, $MAPbX_3$), forming 3D perovskite crystal structures, is a subject of many discussions due to its high photon-to-electron conversion efficiency when used as absorber material, either in bulk hetero junction or planner heterostructure configurations.[3−7] A combination of simplicity in device fabrication and exceptional optoelectronic properties enables it to achieve a paradigm shift in the photovoltaic technology; however, its sensitivity toward moisture plays a detrimental role toward its commercial realization. Much effort has been made in understanding this effect of H_2O on the $MAPbX_3$ structure.[8−13] Initially it was found that on absorption of water the perovskite structure underwent an irreversible decomposition process, resulting in the formation of PbI_2.[9,10,12−14] Recent reports, however, reveal that in the presence of moisture the material may also get hydrated (either mono or di, depending on the exposure time) but has the capability to regain its original structure upon releasing the water molecules.[8,11,15,16]

We explore the dehydration−hydration properties of the dihydrated perovskite, resulting in reversible thermochromic characteristics. The hydration−dehydration process is studied with in situ temperature and time-resolved X-ray diffraction (XRD) and vibration spectroscopy using Fourier transform infrared spectrophotometer (FT-IR). The resultant process is reconnoitered further in the form of photovoltaic device. The performance of the device is found to be highly dependent on ambient conditions and temperature. Such externally stimulated optoelectronic device characteristics can further escalate its realization toward smart window and other building integrated applications.

Thin films of methylammonium iodo-plumbates are prepared by spin-coating a solution containing PbI_2 and CH_3NH_3I (MAI) in *N*,*N*′-dimethylformamide (DMF). The concentration ratio of PbI_2 to MAI in the solution is varied from 1:1 to 1:4. Porous TiO_2 coated on FTO glass or microscopic glass is used as the substrate unless stated otherwise. All processes are performed under ambient conditions with relative humidity ranging between 60 to 70%. Upon spin-casting, the material thus formed on the substrates is subsequently annealed at 90 °C for 15 min, which results in the formation of deep dark-brown color film. Interestingly, gradual discoloration is observed in some films with time when they are cooled to room temperature. It is found that this phenomenon pertains only to those thin film substrates where the relative molar concentration of MAI is higher than that of PbI_2. Without much surprise, no such discolorations are observed for the material prepared with an equi-molar solution of MAI and PbI_2. Fascinatingly it is found that the films prepared from the precursor solution consisting of 1:4 molar concentration of PbI_2 to MAI turned completely transparent within 30 s of exposure to ambient condition as a result of gradual cooling; however, upon reheating to ~60 °C, the brown coloration reappeared, and to the naked eye the films look to be similar to a freshly annealed sample. Here we refrain ourselves from finding the exact temperature at which the coloration reappears,

Received: July 6, 2015
Accepted: July 31, 2015

DOI: 10.1021/acs.jpclett.5b01426
J. Phys. Chem. Lett. 2015, 6, 3180−3184

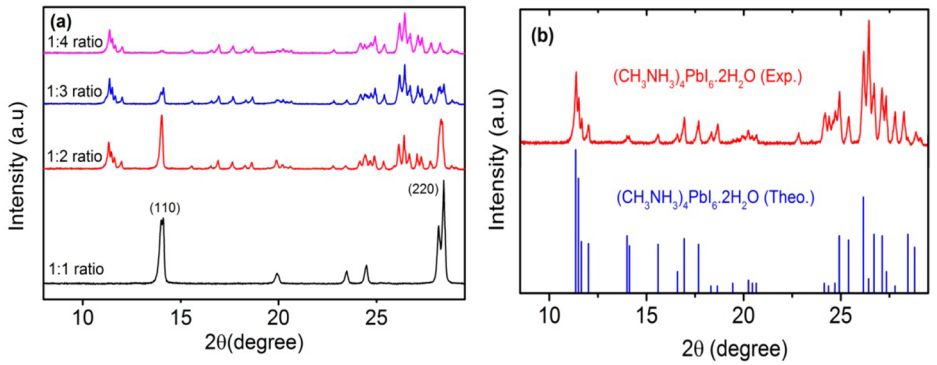

Figure 1. (a) Experimentally obtained XRD patterns of perovskite formed using different ratio of PbI_2 and MAI from 1:1 to 1:4. (b) Comparison between experimentally obtained XRD pattern of 1:4 perovskite resulting in $(CH_3NH_3)_4PbI_6{\cdot}2H_2O$ at room temperature and theoretically calculated XRD pattern of the same by Leguy et. al.[11]

but considering the need for consistency and reproducibility, we keep the reference temperature as 60 °C.

To investigate any possible crystallographic phase change that may be associated with the said thermochromic behavior, we investigate the transition with XRD measurements. All measurements are performed under θ-2θ configuration using Cu Kα radiation (1.54 Å). Materials are prepared in the form of powder with PbI_2 to MAI ratio ranging from 1:1 to 1:4 that are subsequently annealed at 90 °C, followed by gradual cooling to room temperature. The XRD pattern of 1:1 perovskite at room temperature shows the material to have tetragonal structure of $MAPbI_3$, as shown in the Figure 1a. Interestingly it is found that with further increase in the molar concentration of MAI, the XRD patterns deviate largely from the original $MAPbI_3$ structure. The material prepared with PbI_2/MAI of 1:2 shows the appearance of several new peaks along with the characteristic peaks of $MAPbI_3$ perovskite, as also depicted in the Figure 1a. Increasing the MAI concentration still further decreases the characteristic $MAPbI_3$ peak intensities, which completely disappear in the material formed using 1:4 (PbI_2:MAI) precursor, leaving behind only the newly developed peaks. This acquired diffraction pattern has a close resemblance with the theoretically obtained pattern of the $(CH_3NH_3)_4PbI_6{\cdot}2H_2O$ perovskite, calculated and previously reported by Leguy et al.[11] (as shown in Figure 1b). The crystal structure of the dihydrated perovskite is found to be similar to a distorted NaCl structure, consisting of $[PbI_6]^{4-}$ octahedra and surrounded by $(CH_3NH_3{\cdots}H_2O{\cdots}CH_3NH_3)_2^{-4}$.[15] It is to be noted that there is a considerable structural dissimilarity between the mono- and dihydrated $MAPbI_3$ perovskite.[11,16]

The temperature dependent behavioral change of dihydrated perovskite is studied in situ with X-ray diffraction technique. As a base measurement, we first studied the XRD pattern of $MAPbI_3$ that shows tetragonal to cubic phase change upon heating up to 60 °C, a well-known phenomenon previously reported[17] (Figure S1a in the Supporting Information (SI)). From the temperature-resolved XRD measurements (as shown in Figure S1b in the SI), it is clear that the dihydrated perovskite ($(MA)_4PbI_6{\cdot}2H_2O$) goes through a phase transition at 60 °C, probably by releasing the loosely bound water. It is found that at the said temperature the dihydrated perovskite is transformed to the cubic phase of the $MAPbI_3$ perovskite with a few additional peaks at 9.76, 19.59, 26.2, and 23.58°. These peaks basically belong to pure MAI at that particular temperature (Figure 2). Figure 2 shows a comparison of the XRD patterns of dihydrated perovskite, $MAPbI_3$ perovskite,

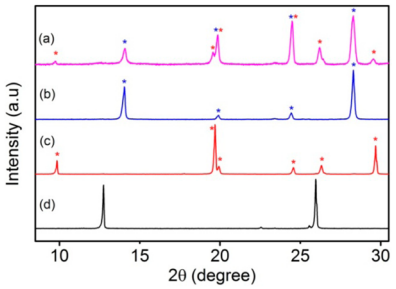

Figure 2. Powder X-ray diffraction patterns acquired at 60 °C for (a) $(MA)_4PbI_6{\cdot}2H_2O$ perovskite, (b) $MAPbI_3$ perovskite, (c) MAI, and (d) PbI_2.

only MAI, and pure PbI_2 all at 60 °C to obtain a clearer idea about the crystallographic differences of the materials at the said temperature. Upon gradual cooling, the material again recrystallizes back to $(MA)_4PbI_6{\cdot}2H_2O$ by absorbing water molecules from the atmosphere, as shown in Figure 3a. This reversible phase change (hydration and dehydration of perovskite) over 10 heating−cooling cycles is shown in Figure 3b.

This phase transformation is, however, found to be unidirectional when the process cycle is performed under vacuum or under inert condition. Under vacuum, when $(MA)_4PbI_6{\cdot}2H_2O$ is heated to 60 °C the material is transformed to $MAPbI_3$ and MAI but never gets reversed back to its original hydrated form, as shown by the in situ time and temperature-resolved XRD measurements (Figure S2, SI). A similar observation is made when the material is synthesized inside the glovebox (inert condition), where it never transforms to the optically transparent state as previously discussed.

To investigate the contribution of ambient humidity on the reversible thermochromic process, we performed in situ FTIR spectroscopy. Here the sample is heated inside the spectrophotometer under ambient condition. The IR spectra (Figure 4, spectrum "a") of $(MA)_4PbI_6{\cdot}2H_2O$ clearly shows the presence of O−H stretch around 3500 cm^{-1} along with other chemical signatures common to $MAPbI_3$. However, the complete removal of the O−H signature peak is seen when the perovskite is heated to 60 °C (Figure 4, spectrum "b"). The O−H signature peak reappears again when the perovskite material is cooled to room temperature under ambient conditions, as indicated in the spectrum "c" of Figure 4. This convincingly proves the role of ambient humidity in achieving a

DOI: 10.1021/acs.jpclett.5b01426
J. Phys. Chem. Lett. 2015, 6, 3180−3184

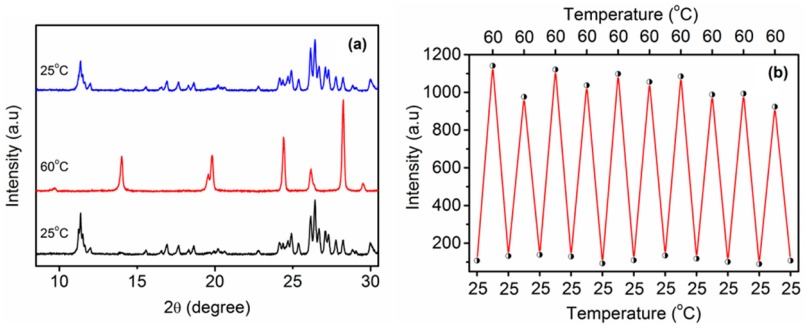

Figure 3. (a) XRD pattern depicting the reversible nature of $(CH_3NH_3)_4PbI_6{\cdot}2H_2O$ to $MAPbI_3$ and MAI upon annealing from 25 to 60 °C and again cooling back to 25 °C. (b) Intensity count of the $MAPbI_3$ signature peak at 28.8° at different temperatures, elucidating the reversible nature of the dihydrated perovskite material through 10 cycles.

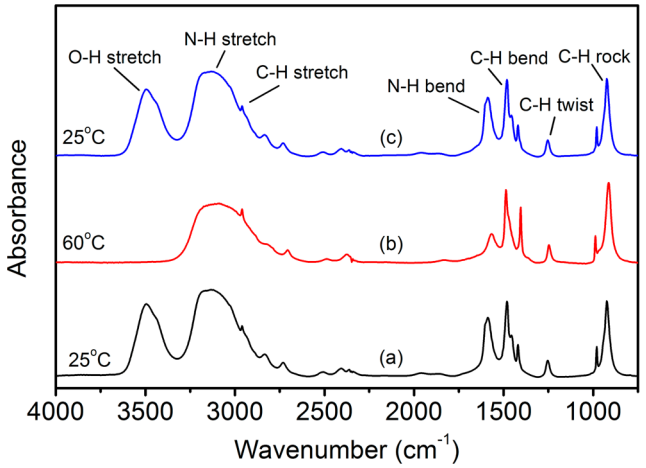

Figure 4. FTIR spectrum shows the appearance and disappearance of OH stretch on heating and cooling the material, thus revealing the role of moisture in achieving the thermochromic perovskite ($(MA)_4PbI_6{\cdot}2H_2O$).

reversible thermochromic behavior in hydrated organic–inorganic hybrid perovskites.

As discussed previously, beyond the equi-molar solution, with increasing MAI concentration in the precursor solution, the material crystallizes as $(MA)_4PbI_6{\cdot}2H_2O$ along with $MAPbI_3$ under ambient condition. We believe that the excess MAI present in the material transforms adequate number of $MAPbI_3$ components to $(MA)_4PbI_6{\cdot}2H_2O$ by absorbing water molecules from air, while the remaining $MAPbI_3$ components are left unchanged as $MAPbI_3$ (as seen previously in Figure 1a,b). As the amount of excess MAI increases to four times of the lead iodide (PbI_2), the excess MAI converts the entire $MAPbI_3$ component to the hydrated $(MA)_4PbI_6{\cdot}2H_2O$ component. This is simply due to the fact that the stoichiometry required to form pure hydrated perovskite is fulfilled when PbI_2 and MAI is mixed in 1:4 molar ratio.

$$4CH_3NH_3I + PbI_2 \rightarrow CH_3NH_3PbI_3 + 3CH_3NH_3I$$
$$\xrightarrow{H_2O} (CH_3NH_3)_4PbI_6{\cdot}2H_2O$$

From these above experiments it is perceived that in the presence of sufficiently excess MAI, $(MA)_4PbI_6.2H_2O$ is found to be a more stable crystal structure than $CH_3NH_3PbI_3$ under humid condition. Thus, it can be said that on heating of dihydrated perovskite, spatially localized $MAPbI_3$ and MAI is formed due to removal of water molecules from the perovskite as Vincent et al. previously stated.[15]

$$(CH_3NH_3)_4PbI_6{\cdot}2H_2O \overset{\Delta}{\leftrightarrow} CH_3NH_3PbI_3 + 3CH_3NH_3I + H_2O\uparrow$$

Figure 5a shows the UV–vis absorption spectra of the $MAPbI_3$ and $(MA)_4PbI_6{\cdot}2H_2O$ films measured at two different temperatures, 60 and 25 °C. As observed, the $MAPbI_3$ perovskite remains persistent with their dark deep brown color, whether heated at 60 °C or at room temperature. The experimentally determined bandgap (from tauc plot) of the stoichiometric $MAPbI_3$ material is found to be 1.58 eV, which is similar to the earlier reported value (~1.6 eV).[2,18,19] However, the dihydrated perovskite shows a significant change in the absorption spectra at 60 °C in comparison with 25 °C, as

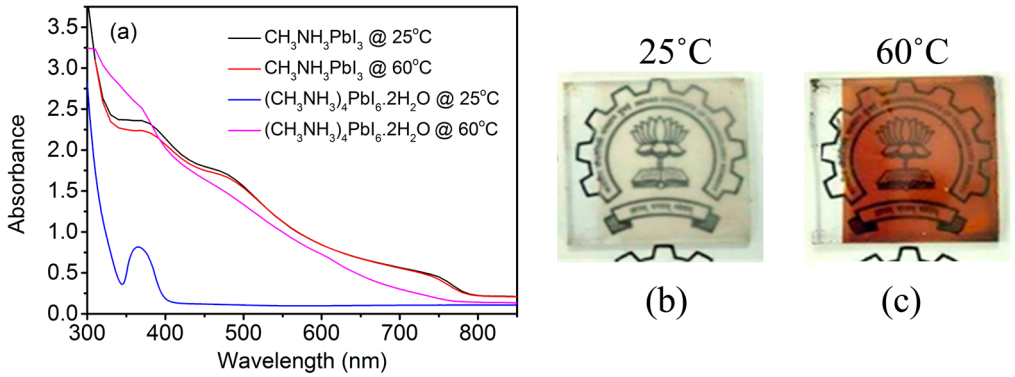

Figure 5. UV–vis absorption spectra of thin films of $MAPbI_3$ and $(MA)_4PbI_6{\cdot}2H_2O$ at 25 and 60 °C. The corresponding image of the thin film of dihydrated perovskite at 25 (b) and at 60 °C (c) is also presented.

DOI: 10.1021/acs.jpclett.5b01426
J. Phys. Chem. Lett. 2015, 6, 3180–3184

shown in Figure 5a. A clear understanding of the color change is depicted in Figure 5b,c. At room temperature the band gap of the $(MA)_4PbI_6{\cdot}2H_2O$ perovskite is measured to be ~3.82 eV, whereas at elevated temperature it is found to be 1.8 eV. The room-temperature bandgap of the material is in close agreement with that reported by Papavassiliou et al. (3.87 eV).[20] Another noteworthy feature of the dihydrated perovskite is the appearance of the second absorption peak at ~370 nm at room temperature. A splitting of the excitonic peak is previously observed for the lower dimension perovskites (2D, 1D, and 0D), probably due to lower symmetry of the crystal field that rises at low temperature.[21] A similar observation on $(MA)_4PbI_6{\cdot}2H_2O$ perovskite (0D) reported a second excitonic peak at 372 nm, which is close to our observed value.

The reversible thermochromic property due to the phase transformation of $(MA)_4PbI_6{\cdot}2H_2O$ is further applied in photovoltaics. The devices are made with porous TiO_2 as electron transport layer and spiro-OMeTAD as hole-conducting layer, while $(MA)_4PbI_6{\cdot}2H_2O$ is used as absorber layer. Figure 6 shows the photovoltaic performance of the device at

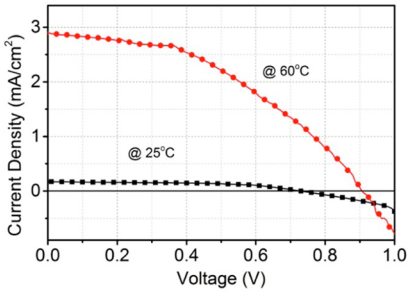

Figure 6. Illuminated $J-V$ characteristics of a thermochromic perovskite-based device at room temperature (25 °C) and at 60 °C.

25 and 60 °C. On heating at 60 °C, the device shows a photon to electron conversion efficiency of 1.2% with open-circuit potential (V_{OC}) of 910 mV and short-circuit current density (J_{SC}) of 2.88 mA/cm^2. On the contrary, at 25 °C they are highly transparent with no significant power conversion. Such thermochromic behavior is often lucrative for building integrated photovoltaic applications. The variation in device performance over five heating cooling cycles is depicted in SI Figure S3. Over repeated annealing cycles, ~20% reduction in device efficiency is observed, but the open-circuit voltage almost remains constant throughout, and the fill factor of the device actually improves to some extent. A major part of the loss is attributed to the decrease in short-circuit current density of the device, which may be due to repeated phase transition in the material. Further optimization for the device fabrication is, however, needed get improved efficiencies.

We reveal direct synthesis of dihydrated $MAPbI_3$ thin films under ambient conditions. At room temperature and in the presence of excess MAI, the rapid formation of dihydrated perovskite suggests the stable nature of this hydrated perovskite structure. The reversible thermochromic behavior through the dehydration-hydration process of $(CH_3NH_3)_4PbI_6{\cdot}2H_2O$ is explored. A change in bandgap from 3.82 to 1.80 eV is experimentally determined when the material is heated to 60 °C. The presence of water vapor or humidity is found to be the necessary condition for this temperature-dependent phase change of the dehydrated perovskite system. The thermochromic nature of the material is further utilized in photovoltaic devices, resulting in modest power conversion efficiencies, opening an avenue to be utilized in building integrated devices.

EXPERIMENTAL SECTION

Material Required. Hydroiodic acid (Sigma-Aldrich, 57 wt % in water), methylamine (Sigma-Aldrich, 33 wt % in absolute ethanol), lead iodide (Sigma-Aldrich, 99.5%), fluorine-doped tin-oxide-coated glass (Pilkington, TEC-8), titanium isopropoxide (Sigma-Aldrich, > 97%), titania (Dysol, 18NRT paste), alumina nanoparticle dispersion in iso-propanol (Sigma-Aldrich, > 50 nm), spiro-OMeTAD (Lumtec), Li-TFSI (Sigma-Aldrich), *tert*-butylpyridine (Sigma-Aldrich, 98%), chlorobenzene (Sigma-Aldrich, 99.9%), and silver metal (Parekh Industries, 99.9%) are used without further processing for material formation and device fabrication.

Synthesis of Methylammonium Iodide. The methylammonium iodide is synthesized by mixing of equimolar concentration of methylamine and hydroiodic acid at 0 °C for 2 h. The methylammonium iodide salt is obtained by evaporating the solvent from the solution using rotary evaporator. The recovered salt is then dissolved in ethanol and recrystallized from diethyl ether and washed with diethyl ether for few times. The recrystallized salt is then dried in a vacuum oven for 12 h at 50 °C.

Sample Preparation for FTIR Measurement. Potassium bromide (KBr) pellets coated with Al_2O_3 by atomic layer deposition (ALD) are used as substrates for in situ FTIR experiments. The perovskite precursor solutions are drop casted on the ALD-Al_2O_3-coated KBr pellets and annealed at 90 °C to form films. The perovskite-coated pellets are then immediately used for experiments.

Sample Preparation for UV−vis Measurement. Quartz substrates cleaned with alconox soap solution, followed by iso-propanol, acetone, and double-distilled water are used. As-received Al_2O_3 dispersion is diluted and spin-coated on the quartz substrates and annealed at 150 °C for 30 min. The perovskite films are prepared by spin coating the precursor solution of different proportion of PbI_2 and MAI on the Al_2O_3-coated quartz substrates. The films are then annealed at 90 °C for 15 min and immediately used for the experiments.

Device Fabrication. The FTO-coated glasses are patterned using zinc powder and dilute hydrochloric acid and cleaned by alconox soap, followed by iso-propanol, acetone, diluted sodium hydroxide, and double-distilled water. The dense TiO_2 layer is made from titanium isopropoxide solution as per the procedure provided by Docampo et.al.[22] This precursor solution is spin-coated on the cleaned FTO glass at 2000 r.p.m. for 30 s, and the TiO_2-coated substrates are subsequently annealed at 500 °C for 1 h. A layer of porous TiO_2 is deposited on top of the dense TiO_2 film by spin coating the diluted dyesol-TiO_2 paste at 2000 r.p.m. to 60 s, followed by sintering at 500 °C for 1 h. To make the thermochromic perovskite layer, a precursor solution consisting of 1:4 molar ratio of PbI_2 to MAI is spin-coated on top of the porous TiO_2 film and annealed at 90 °C for 15 min in an inert environment. The perovskite-coated substrate is gradually cooled to room temperature and coated with Li-TFSI-doped Spiro-OMeTAD solution, as reported by Burschka et al.[5] The top contact of the device is made by thermal evaporation of silver with a thickness of 100 nm.

XRD, UV−vis, FTIR, and J−V Measurement. Temperature and time-resolved X-ray diffraction measurements are performed using Rigaku smart lab XRD instrument. The UV−vis

DOI: 10.1021/acs.jpclett.5b01426
J. Phys. Chem. Lett. 2015, 6, 3180−3184

measurements are carried out on PerkinElmer LAMBDA 950 spectrophotometer. The high-temperature measurements are executed by heating the substrates on a hot plate and placing them immediately for measurement. Vertex 70 FTIR instrument from Bruker is used to conduct the in situ FTIR measurements. All spectra were acquired over an average of 100 scans with a resolution of 4 cm^{-1}. For current voltage characterization, a xenon lamp calibrated to 1000W/m^2 intensity is used as the light source, and the cell active area is kept to be 0.09 cm^2 by using a metal mask.

■ ASSOCIATED CONTENT

Ⓢ Supporting Information

The Supporting Information is available free of charge on the ACS Publications website at DOI: 10.1021/acs.jpclett.5b01426.

Additional XRD patterns and details of device performances (PDF).

■ AUTHOR INFORMATION

Corresponding Author

*E-mail: shaibal.sarkar@iitb.ac.in.

Notes

The authors declare no competing financial interest.

■ ACKNOWLEDGMENTS

We thank the National Center for Photovoltaic Research and Education aided by the Ministry of New and Renewable Energy, Govt. of India, for financial support.

■ REFERENCES

(1) Mitzi, D. B.; Chondroudis, K.; Kagan, C. R. Organic-Inorganic Electronics. *IBM J. Res. Dev.* **2001**, *45*, 29−45.

(2) Butler, K. T.; Frost, J. M.; Walsh, A. Band Alignment of the Hybrid Halide Perovskites $CH_3NH_3PbCl_3$, $CH_3NH_3PbBr_3$ and $CH_3NH_3PbI_3$. *Mater. Horiz.* **2015**, *2*, 228−231.

(3) Lee, M. M.; Teuscher, J.; Miyasaka, T.; Murakami, T. N.; Snaith, H. J. Efficient Hybrid Solar Cells based on Meso-Superstructured Organometal Halide Perovskites. *Science* **2012**, *338*, 643−647.

(4) Kim, H.-S.; Lee, C.-R.; Im, J.-H.; Lee, K.-B.; Moehl, T.; Marchioro, A.; Moon, S.-J.; Humphry-Baker, R.; Yum, J.-H.; Moser, J. E.; Grätzel, M.; Park, N.-G.; et al. Lead Iodide Perovskite Sensitized All-Solid-State Submicron Thin Film Mesoscopic Solar Cell with Efficiency Exceeding 9%. *Sci. Rep.* **2012**, *2*, 591.

(5) Burschka, J.; Pellet, N.; Moon, S.-J.; Humphry-Baker, R.; Gao, P.; Nazeeruddin, M. K.; Gratzel, M. Sequential Deposition as a route to High-Performance Perovskite-Sensitized Solar Cells. *Nature* **2013**, *499*, 316−319.

(6) Heo, J. H.; Im, S. H.; Noh, J. H.; Mandal, T. N.; Lim, C.-S.; Chang, J. A.; Lee, Y. H.; Kim, H.-J.; Sarkar, A.; Nazeeruddin, Md. K.; Grätzel, M.; Seok, S. I.; et al. Efficient Inorganic-Organic Hybrid Heterojunction Solar Cells containing Perovskite compound and Polymeric Hole Conductors. *Nat. Photonics* **2013**, *7*, 486−491.

(7) Liu, D.; Kelly, T. L. Perovskite Solar Cells with a Planar Heterojunction structure prepared using Room-Temperature Solution Processing Techniques. *Nat. Photonics* **2013**, *8*, 133−138.

(8) Christians, J. A.; Miranda Herrera, P. A.; Kamat, P. V. Transformation of the Excited State and Photovoltaic Efficiency of $CH_3NH_3PbI_3$ Perovskite upon Controlled Exposure to Humidified Air. *J. Am. Chem. Soc.* **2015**, *137*, 1530−1538.

(9) Frost, J. M.; Butler, K. T.; Brivio, F.; Hendon, C. H.; van Schilfgaarde, M.; Walsh, A. Atomistic Origins of High-Performance in Hybrid Halide Perovskite Solar Cells. *Nano Lett.* **2014**, *14*, 2584−2590.

(10) Han, Y.; Meyer, S.; Dkhissi, Y.; Weber, K.; Pringle, J. M.; Bach, U.; Spiccia, L.; Cheng, Y.-B. Degradation observations of Encapsulated Planar $CH_3NH_3PbI_3$ Perovskite Solar Cells at High Temperatures and Humidity. *J. Mater. Chem. A* **2015**, *3*, 8139−8147.

(11) Leguy, A. M. A.; Hu, Y.; Campoy-Quiles, M.; Alonso, M. I.; Weber, O. J.; Azarhoosh, P.; van Schilfgaarde, M.; Weller, M. T.; Bein, T.; Nelson, J.; Docampo, P.; et al. Reversible Hydration of $CH_3NH_3PbI_3$ in Films, Single Crystals, and Solar Cells. *Chem. Mater.* **2015**, *27*, 3397−3407.

(12) Niu, G.; Li, W.; Meng, F.; Wang, L.; Dong, H.; Qiu, Y. Study on the Stability of $CH_3NH_3PbI_3$ Films and the Effect of Post-Modification by Aluminum Oxide in All-Solid-State Hybrid Solar Cells. *J. Mater. Chem. A* **2014**, *2*, 705−710.

(13) Yang, J.; Siempelkamp, B. D.; Liu, D.; Kelly, T. L. Investigation of $CH_3NH_3PbI_3$ Degradation Rates and Mechanisms in Controlled Humidity Environments Using in Situ Techniques. *ACS Nano* **2015**, *9*, 1955−1963.

(14) Mosconi, E.; Azpiroz, J. M.; De Angelis, F. Ab initio Molecular Dynamics Simulations of $MAPbI_3$ Perovskite Degradation by Water. *Chem. Mater.* **2015**, *27*, 4885−4892.

(15) Vincent, B. R.; Robertson, K. N.; Cameron, T. S.; Knop, O. Alkylammonium Lead Halides. Part 1. Isolated PbI_6^{4-} ions in $(CH_3NH_3)_4PbI_6{\bullet}2H_2O$. *Can. J. Chem.* **1987**, *65*, 1042−1046.

(16) Imler, G. H.; Li, X.; Xu, B.; Dobereiner, G. E.; Dai, H.-L.; Rao, Y.; Wayland, B. B. Solid State Transformation of the Crystalline Monohydrate $(CH_3NH_3)PbI_3(H_2O)$ to the $(CH_3NH_3)PbI_3$ Perovskite. *Chem. Commun.* **2015**, *51*, 11290−11292.

(17) Baikie, T.; Fang, Y.; Kadro, J. M.; Schreyer, M.; Wei, F.; Mhaisalkar, S. G.; Graetzel, M.; White, T. J. Synthesis and Crystal Chemistry of the Hybrid Perovskite $(CH_3NH_3)PbI_3$ for Solid-State Sensitised Solar Cell Applications. *J. Mater. Chem. A* **2013**, *1*, 5628−5641.

(18) Umari, P.; Mosconi, E.; De Angelis, F. Relativistic GW calculations on $CH_3NH_3PbI_3$ and $CH_3NH_3SnI_3$ Perovskites for Solar Cell Applications. *Sci. Rep.* **2014**, *4*, 4467.

(19) Ziang, X.; Shifeng, L.; Laixiang, Q.; Shuping, P.; Wei, W.; Yu, Y.; Li, Y.; Zhijian, C.; Shufeng, W.; Honglin, D.; Minghui, Y.; Qin, G. G. Refractive Index and Extinction Coefficient of $CH_3NH_3PbI_3$ studied by Spectroscopic Ellipsometry. *Opt. Mater. Express* **2015**, *5*, 29−43.

(20) Koutselas, I. B.; Ducasse, L.; Papavassiliou, G. C. Electronic properties of Three- and Low-Dimensional Semiconducting Materials with Pb Halide and Sn Halide units. *J. Phys.: Condens. Matter* **1996**, *8*, 1217.

(21) Papavassiliou, G. C. Three- and Low-Dimensional Inorganic Semiconductors. *Prog. Solid State Chem.* **1997**, *25*, 125−270.

(22) Docampo, P.; Ball, J. M.; Darwich, M.; Eperon, G. E.; Snaith, H. J. Efficient Organometal Trihalide Perovskite Planar-Heterojunction Solar Cells on Flexible Polymer substrates. *Nat. Commun.* **2013**, *4*, 2761.

DOI: 10.1021/acs.jpclett.5b01426
J. Phys. Chem. Lett. 2015, 6, 3180−3184